Enhancing Quantitative Precision and Accuracy in Complex 'Systems' utilizing Advanced Informatics and a Highly Selective and Orthogonal Analytical Workflow

Roy Martin[1], Brent Martin[2], Chris Hughes[3], James Langridge[3], Scott Geromanos[1],
[1] Waters Corporation, Milford, MA, [2] University of Michigan, Ann Arbor, MI, [3]Waters Corporation, Manchester, United Kingdom

INTRODUCTION

The ability to accurately determine the quantitative change of any molecular ion between two or more complex "systems" is predicated on how well each ion has been measured. How well each ion is measured relates directly to the peak capacity, selectivity and specificity of the employed analytical workflow. Selectivity relates to the methods ability to measure the physiochemical attributes [*m/z*, retention time (t_r), drift time (t_d), peak area] of each ion independent of all others while specificity reflects the precision of each measurement.

Presented is how the inclusion of Ion Mobility Separation (IMS) into the analytical workflow promotes peak capacity, selectivity and specificity culminating in greater quantitative accuracy and precision across the widest dynamic range.

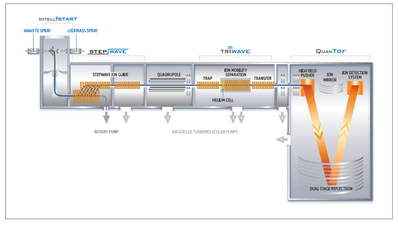

Figure 1. Synapt G2-S Ion Mobility Enabled Mass Spectrometer. The Ion Mobility Separation is performed in the TriWave region.

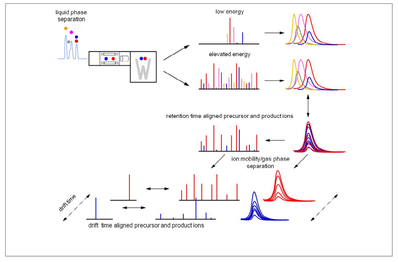

Figure 2. LC-IM-DIA-MS (HDMS^E) scanning method.

METHODS

Sample preparation

Yeast strain W303 MATα (ATCC:24657) (Blue Sky BioServices, Worcester, MA) was grown in YPD medium until early- to mid-log phase. MDA-MB-231 cells were cultured in DMEM (4.5 g/liter glucose)-based medium with 10% dialyzed fetal bovine serum fro 10 cell cycles. SILAC labeling and enzymatic digestion was performed as previously described[1]. All protein samples were lysed in 7 M urea, 2 M thiourea and 50 mM ammonium bicarbonate lysates were centrifuged at 13,000 rpm for 20 min. Protein concentrations were estimated using a Bradford protein assay kit (Bio-Rad, Hercules, CA).

LC-MS conditions

Samples were analyzed in triplicate using a nanoACQUITY coupled to a Synapt G2-S mass spectrometer, **Figure 1**. 1 µ L (~100ngram) of each sample was loaded on a 1.8 µm HSS T3 75 µm x 150 mm column. Peptides were eluted using a gradient of 99% A (0.1% (v/v) formic acid) 1% B (99.9% acetonitrile 0.1% (v/v) formic acid) to 40% B over 90 min at 300 nL/min. Data was acquired by MS^E with and without IMS activated **Figure 2**.

Data analysis

A developmental version of ProteinLynx GlobalSERVER (Waters Corporation) was used to process both the LC-MS^E and LC-HDMS^E datasets. After some smoothing, fitted Gaussians were applied to the raw ion signals in each of the 3 dimensions of *m/z*, retention (t_r) and drift (t_d). Local maxima were calculated and recorded. In addition, each of the 3 attribute were assigned their respective full-width at half height ($W_{0.5}$). An experimental resolution or $R_{x\,effective}$ was calculated for each ion dividing the centered *m/z* by its measured $W_{0.5}$. Utilizing the Lock Spray channel, the TOF mass resolution is monitored across the entire gradient elution and median value calculated. Similarly, median $W_{0.5}$ values are calculated for both t_r and t_d. Utilizing these median values a purity score is calculated for each attribute. **Figure 3**. The final *ion* purity score is a weighted average of each of the individual scores. The ion selection criteria for calculating both the quantitative change and associated error is determined by the distribution of the final ion purity scores.

Figure 3.

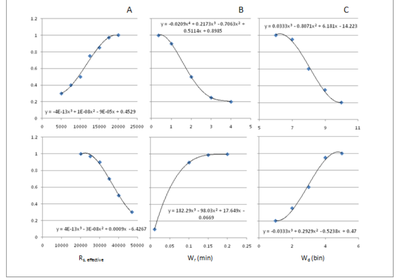

RESULTS

SILAC Labeling

In a binary SILAC experiment how pervasive is ion interference? Figure 4 reflects what happens when the 'light' and 'heavy' samples are combined. Table 1 reports the total number of ion detections for each variant analyzed independently

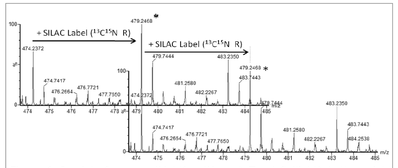

Figure 4. Ion interference - 'Light' v. 'Heavy'. Top left 'light', bottom right 'heavy'. As examples mixed the 2⁺ ion of m/z 474.2372 labeled interferes with the 2⁺ 'light' of m/z 479.2458. Additionally, the same 2⁺ ion when labeled interferes with the 'light' ion at m/z 484.2538. Separation would require >100K mass resolution.

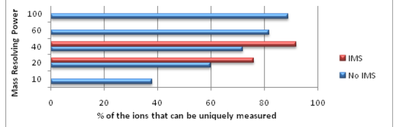

Figure 5. 750K unique peptide sequences from the UniProt db of H. sapiens (39,928 entries, release 3.85) were represented as 12 m/z values ($A_{0,1,2}$ of CS_{1-4}) each assigned tr (SSRCalc²) and a td (Valentine et.al³). Each was queried at +/-, 15 secs, 0.5 drift and the Δ mass at half -height for mass resolutions of 10,20,40,60 & 100K to calculate what % of the over 7.5x10⁶ ions could be uniquely measured. For the two operating resolutions of the G2-S, IMS was included.

Ion interference rates, illustrated in **Table 1**. are predicated on the assumption that prior to the 'heavy' label all ion detections are unique, which does not have to be the case and will be explored later in the label-free section. **Table 1**. does illustrate that the number of ion detections, AMRTs and matched pairs increases at average rates of 21.2%, 16.8% and 15.4%, respectively, with IMS employed. The number of ion interference events dropped from on average 20.2% to 5.4%.

Figure 6.

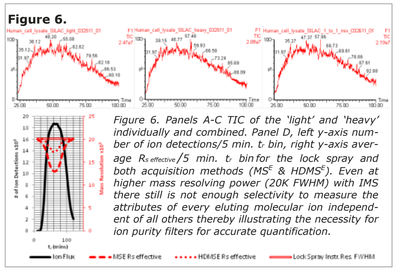

Figure 6. Panels A-C TIC of the 'light' and 'heavy' individually and combined. Panel D, left y-axis number of ion detections/5 min. t_r bin, right y-axis average $R_{x\,effective}$/5 min. t_r bin for the lock spray and both acquisition methods (MS^E & HDMS^E). Even at higher mass resolving power (20K FWHM) with IMS there still is not enough selectivity to measure the attributes of every eluting molecular ion independent of all others thereby illustrating the necessity for ion purity filters for accurate quantification.

Table 1.

Sample	# ion detections (x10⁶)		# AMRTs (x10⁶)		# peptides		# proteins	
	MS^E	HDMS^E	MS^E	HDMS^E	MS^E	HDMS^E	MS^E	HDMS^E
light	170.5 (19.3%)*	217.5 (5.2%)*	39.3 (7.5%)*	49.9 (3.5%)*	4965	8258	558	842
heavy	182.4 (21.2%)*	221.2 (5.7%)*	40.3 (8.3%)*	51.2 (3.9%)*	5126	8381	562	868
mixed	328.2 (69.5%)**	404.9 (82.1%)**	33.2 (15.2%)**	44.5 (21.2%)**	4137	6985	452	680

* common in 'light' and 'heavy' datasets ** ions and AMRTs illustrating a 'light-heavy' pair

Examination of both the number and interference rate of AMRTs for both acquisition methods illustrates a similar trend, with the number of AMRTs increasing on average 23.6% with IM enabled, at the same time the percent of AMRTs occupying the same mass and time dropped on average from 7.9% to 3.7%. Since the sample being analyzed is the same, the difference in the number of ion detections and ion interference events can be solely ascribed to the inclusion of the orthogonal on-line IM separation. Moreover, the addition of IM provides for more selective precursor-product ion alignment in that precursor and product ions are aligned by both t_r and t_d. This increased selectivity resulted in an average increase of 64.3% and 50.2% respectively in the number of peptides and proteins identified with IM incorporated into the applied analytical workflow.

To provide insight into how interfering ion events ultimately affect quantitative performance, **Figure 5** illustrates log-log plots of the calculated ion areas of matched 'light' and 'heavy' variants for the MDA-MB-231 cells diluted 1:1, 1:5 and 1:10 respectively. **Figure 6.** illustrates the average area ratios of 'heavy' to 'light' variants across the matched dynamic range of the 'heavy'. From this point on grey circles and bars represent ion pairs that have passed the ion purity filter, whereby black represent those that did not. Given the previous results only the LC-HDMS^E data is presented. **Figure 6** panels A-C clearly illustrate the increase in quantitative accuracy when the ion purity filters are employed.

Figure 5.

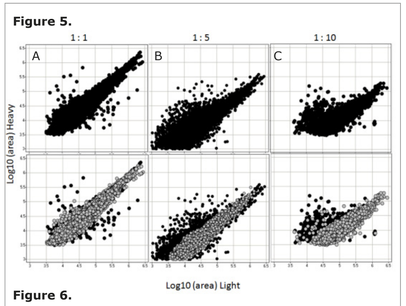

Figure 6.

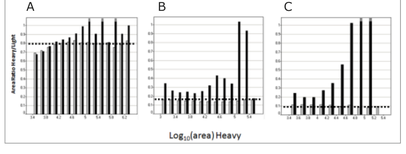

Label-Free

Figure 7 A & B, log-log plots of matched ion areas from replicate injections 100ng yeast lysate. Panel A MS^E, Panel B HDMS^E. Examination of the typical tear-drop shape illustrates a tighter/narrower profile across the entire dynamic range for the HDMS^E data. The insets provide insight into the distribution of calculated ion area ratios from the matched replicates.

Figure 7.

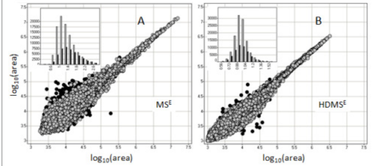

Figure 8.

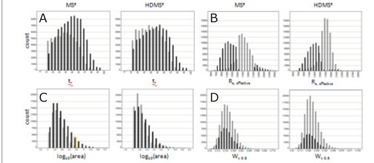

Table 2.

injection	acq. Method	# ion detections	# AMRTs	# peptides	# proteins
1	MS^E	154,856	28,370	4476	538
2	MS^E	162,248	29,011	4665	553
1	HDMS^E	197,248	37,156	6858	902
2	HDMS^E	195,035	37,289	6918	908

Approximately 66.7% of the calculated ratios from the HDMS^E dataset were within ± 15% of nominal with a max. min. of 1.5 and 0.5, respectively. As for the MS^E data, only 42.3% was within an accuracy of ± 15%. **Table 2** summarizes the number of ion detections from each of the two replicate experiments. Similar to the SILAC datasets, on average, the number of ion detections increased ~17% with IMS activated. Given that the sample, column load, gradient, and mass resolution were the same the increase in the number of ion detections can only be attributed to the increased peak capacity afforded by the IM separation. To that end **Figure 8** panel A-D graphically illustrate how IMS affected the overall system-wide peak capacity.

Panels A to D of **Figure 8** reflect the number of ion detections/time, $R_{x\,effective}$ and t_r $W_{0.5}$, left (MS^E), right (HDMS^E). As before, grey ions passing the purity filter, black not. **Panels A** illustrate more ions as passing the purity filter throughout the entire gradient elution with IM employed. Similarly, **Panels B** illustrate a denser, tighter distribution of $R_{x\,effective}$. **Panels C** as expected illustrates a shift in the distribution of ion detections across the experimental dynamic range. By increasing peak capacity lower intensity ions are isolated from higher intensity ions of similar *m/z* and hydrophobicity ergo the shift. Lastly, **Panels D** illustrate a tighter distribution of t_r $P_{0.5}$ with IM employed. As illustrated in **Table 2** the increased peak capacity afforded by the inclusion of the orthogonal IM separation resulted respectively, in a 52% and 67% increase in peptides and proteins identifications.

Figure 9.

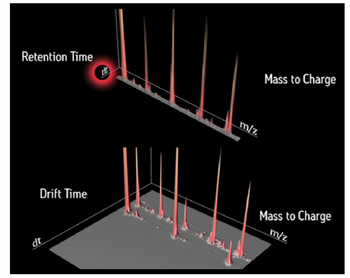

Figure 9. Top—Illustrated is a isotopic cluster of ions whose purity scores in the 3 dimension of $R_{x\,effective}$, t_r $W_{0.5}$ and t_d $W_{0.5}$ when combined result in a final ion purity eliminating them from quantitative consideration. Bottom - same ion series including IM separation—results in a finial ion purity in which all ions are included in the quantitative calculations.

CONCLUSION

- **In the analysis of complex "systems" many perceived unique signals are actually composite signals .**
- **Accurate assessment of quantitative change "requires" knowledge of how precise each ion has been measured.**
- **Un-biased (all ion) HDMS^E acquisitions and advanced informatics provide the means to measure how well each ion has been measured in the 4 measured dimensions of *m/z*, t_r, t_d and area**
- **Ion Purity scores can be utilized to filter which ions are capable of calculating highly accurate quantitative measurements across the widest dynamic ranges**

References

1. Software for quantitative proteomic analysis using stable isotope labeling and data independent acquisition. Mundy Huang, X., Liu, M., Nold, MJ., Kai Fu, T., Zheng, I., Geromanos, SJ., Ding, SJ. *Anal. Chem*. 2011 Aug;83 (18):6971-9.
2. Predicting Peptide Retention Times for Proteomics Krokhin, OV, Spicer, V. *Current Protocols in Bioinformatics*. 2010 Sep;74(9):5391-6.
3. Using ion mobility to improve peptide identification: intrinsic amino acid size parameters. Valentine, SJ., Ewing, AE., Dilger, JM., Glover, MS., Geromanos, SJ., Hughes, C., Clemmer, DE. *Journal of Proteome Research*. 2011 Mar;10 (5):2318-29.

Acknowledgements

Martha Stapels, Keith Fadgen, Steve Ciavarini and Johannes Vissers are kindly acknowledged for their valuable contributions throughout the development of this work.

TO DOWNLOAD A COPY OF THIS POSTER, VISIT WWW.WATERS.COM/POSTERS

Waters
THE SCIENCE OF WHAT'S POSSIBLE.™